JOURNAL OF MATERIALS SCIENCE: MATERIALS IN MEDICINE 7 (1996) 511–516

Nanometre–scale surface features of arthropathic microcrystals and their relation to protein adsorption. A study by scanning probe microscopy and wide angle X-ray diffraction

L. J. GATHERCOLE
H. H. Wills Physics Laboratory, University of Bristol, Bristol BS8 1TL, UK
A. J. SWAN, G. PRICE, P. A. DIEPPE
Rheumatology Unit, University of Bristol, Bristol Royal Infirmary, Bristol BS2 8HW, UK

Crystal preparations cleaned of organic deposits were extracted from cartilage deposits from osteoarthritic (OA) knee joints. These were studied by wide angle X-ray diffraction (WAXD) using a two-dimensional detector in order to ascertain the crystal species composition. Microcrystals in the mixtures were examined by scanning probe microscopy techniques to investigate the form and surfaces of individual particles. This examination resolved surface details on the crystals in the nanometre range. In some hydroxyapatite-rich deposits, small plate-like crystals closely resembling the intrafibrillar hydroxyapatite from calcifying turkey tendon collagen could be seen, suggesting these may have originally formed within collagen fibres. The surface features of triclinic calcium pyrophosphate dihydrate (T-CPPD), which were the predominant species of both synthetic crystals and CPPD from biological deposits, showed areas of relatively regular undulations of the order of 10 nm across and 3 nm deep. Their presence in synthetic crystals confirmed that this roughness, on the scale of a few unit cells, could not have arisen from the biological cleaning process. This suggested a mechanism whereby extra crystal surface could be made available for the location and adhesion of globular proteins, the majority of which tend to be of compatible molecular dimensions. This was tested by incubation of synthetic T-CPPD with human fibronectin, albumin and immunoglobulin G (IgG), followed by washing these free of unbound protein. Re-examination by SPM methods revealed arrays of the proteins located on the crystal surface and this confirmed the binding capacity of such crystals for proteins *in vivo*.

1. Introduction

Osteoarthritis (OA) of the knee joint is one of the most frequent causes of chronic pain and disability in older people [1]. Calcium-containing crystals are frequently found in the cartilage, synovial fluid or synovium of joints with knee OA [1]. Two main types of mineral have been identified: calcium pyrophosphate dihydrate crystals (CPPD), and a variety of forms of basic calcium phosphate (BCP), predominantly apatites [1]. CPPD crystals are thought to form in cartilage (particularly fibrocartilage menisci), and it has been hypothesized that they appear as a result of the increased chondrocyte metabolic activity that accompanies the attempted repair response of the tissue [2, 3]. The biological effects of both BCP and CPPD crystals are mediated by interaction of the crystals with proteins and cell membranes, and protein attachment to the charged particle surfaces is probably a key factor in the pathogenesis of all crystal-related arthropathies [4, 5]. The ability directly to visualise these interactions, with a long-term objective of studying the conditions of protein adhesion and release, would clearly be an important step in the study of crystal related arthropathies and is why we initiated the study.

The relation between osteoarthritis (OA) progression and severity and crystal deposition [6] and in particular the roles of calcium pyrophosphate dihydrate (CPPD) are continuing problems of primary clinical and scientific importance [7]. Biophysical investigations up to now have been hampered by a lack of good preparative techniques, especially for the harvesting and purification of OA crystal deposits and of analytical techniques for use on the crystals, especially for surface related data of high resolution. Recently improved methods of preparation of OA crystal deposits have become available [8, 9]. We decided to combine these with an investigation referring also to pure synthetic CPPD, involving use of a fast recording

0957–4530

wide angle X-ray diffraction technique and scanning probe microscopy (SPM) to look at the composition and detailed surface structure of arthropathic crystals together with their ability to bind proteins.

2. Materials and methods

2.1. Osteoarthritic crystals

These originated from knee joints which showed chronic OA and had been removed at surgery for joint replacement. Crystals were excised from joint tissues: synovium and menisci. The crystals were purified of tissue debris and adsorbed material by the technique of Swan *et al.* [8, 9]. Briefly this involves dicing the tissues, treating them with hyaluronidase, prior to digestion with a 10 mg/ml solution of papain. Protein was broken down and removed by washing in sodium hypochlorite. This procedure provides crystals of widely differing sizes suitable for the SPM and WAXD studies. Nine sets of crystal deposits were examined, originating from right and left synovia, right and left lateral meniscus and right and left medial meniscus

2.2. Triclinic calcium pyrophosphate dihydrate

Synthetic CPPD was made in the rheumatology laboratory using a modification of the gel growth technique [10]. This produced predominantly triclinic crystals, with a minor monoclinic component. The technique has been found to generate triclinic crystals of a 0.1 to 20 μm length, and the study was restricted to this group.

2.3. Protein treatment of synthetic CPPD crystals

100 mg aliquots of CPPD crystals were incubated in a rotating mixer at 37 °C for 30 min in balanced salt solutions containing 1% w/v of either human albumin, fibronectin or IgG. The source of all proteins was Sigma Chemical Co. Ltd., Poole, Dorset. Crystals were recovered from the mixing solution by centrifugation, gently washed in the balanced salt solution, then in deionised distilled water, before SPM examination.

2.4. WAXD technique

We used a Siemens X-1000 two-dimensional wire area detector system for analysing crystal samples. This was mounted on an Elliott GX-21 rotating anode source using a copper anode and a monochromator providing CuK_α radiation in a narrow beam at the specimen. Specimen to detector distances of 5.5 and 8.5 cm were used. Data collection and handling was by the Siemens General Area Detector System (GADDS) software package, run on a 486 pc. The crystal samples were mounted in 0.5 mm diameter glass Lindemann tubes. Air blanks for background subtraction were taken using the same exposures of Lindemann tubes without sample. Using the GADDS package, diffraction patterns could then be background subtracted, geometrically corrected, and the diffraction peaks analysed for position (d-spacing) and intensity.

2.5. Scanning probe microscopies

Both scanning tunnelling microscopy (STM) and scanning force (= atomic force) microscopy (AFM) were employed in the study. A WA Technology (Cambridge UK) scanning tunnelling microscope was used for the STM work and a Nanoscope III (Digital Instruments) for the SFM work. In AFM, both repulsive mode imaging and "tapping mode" imaging were used. In the former mode, the repulsive forces experienced by a cantilever-mounted silicon nitride tip scanned over the specimen surface constitutes the signal which is mapped to position on the specimen. In the latter mode, to minimize the translational forces between specimen and tip, which tend to lead to specimen movement and image distortion, the image is constructed from signals as the tip moves towards and away from the specimen. In the STM the image is constructed from the tunnel current between tip and specimen when the wave functions of electronic states in specimen and probe overlap. This occurs at separations of the order of atomic separations, when a voltage is applied. The instrument was operated in constant current mode, and the signal related to the z direction piezo movement necessary to maintain the set tunnel current [see 11–15]. For image analysis, the package provided on the Nanoscope III was used for both AFM and STM images.

3. Results

3.1. X-ray diffraction

Five-minute exposures were sufficient to obtain an X-ray diffraction 'fingerprint' of each crystalline sample. X-ray diffraction patterns of varying resolution, complexity and information content were recorded from the nine crystal deposits. In a blind test on samples previously characterized in the Rheumatology laboratory, the method could rapidly identify the content of pure HA, pure triclinic CPPD, and mixtures containing HA, triclinic CPPD, and monoclinic CPPD (see Table I). The predominant crystals shapes in each deposit identified by low power SPM techniques were consistent with those identified by optical methods [16]. As expected, triclinic and monoclinic CPPD could be identified in most tissues [17].

3.2. Scanning probe microscopy

The crystal shapes of deposits featured in Table I were consistent with their X-ray diffraction patterns. The right lateral meniscus deposit contained both small plate-like crystals (HA) and elongated flattened tabular entities, some rod-like (CPPD). In the left lateral meniscus deposit these latter shapes predominated, with some stacked plates and more irregular entities. Fig. 1 shows a three-dimensional view of a hydroxyapatite deposit from a mixed crystal deposit in a lateral meniscus. The deposits of about 100 nm each are

TABLE I Analysis of crystal deposit WAXD patterns using the GADDS *peaks* program (identification of T-CPPD reflections in a CPPD rich and a complex OA deposit)

Xtal	from	Reflections (nm)																
Rlm	OA	0.227	0.230	0.266	0.278		0.311 (s)	0.325 (s)	0.346		0.379		0.411		0.464		0.558	0.705 (s)	0.800 (s)
Lmm	OA				0.281		0.312 (s)	0.328 (s)		0.350	0.378	0.408					0.557	0.702 (s)	0.802 (s)
HA	syn.				0.278 (s)	0.308			0.344 (s)										
TCPPD	syn.						0.314 (s)	0.325 (s)		0.352		0.405	0.412	0.446		0.525	0.551	0.698 (s)	0.801 (s)

Rlm: Right lateral meniscus crystal deposit from OA knee–complex by SPM including visible CPPD and HA.
Lmm: Left medial meniscus crystal deposit from OA knee–CPPD rich by SPM.
TCPPD: Pure synthetic triclinic calcium pyrophosphate dihydrate. HA: synthetic hydroxyapatite.
The strongest reflections are designated (s).

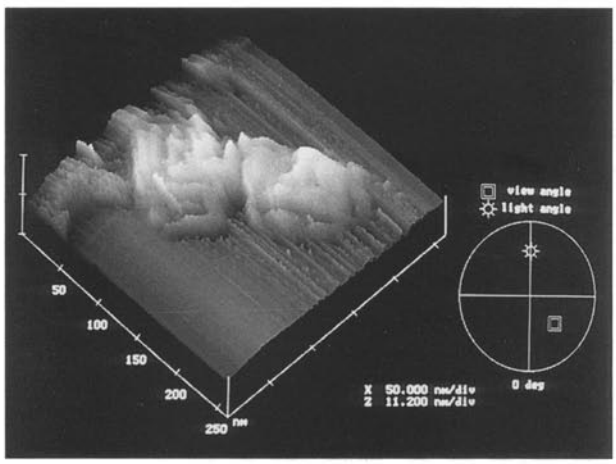

Figure 1 STM image of a HA microcrystal cluster in a mixed specimen from OA r. lateral meniscus deposit. Surface plot. 0.1 nA tunnel current, 800 mV bias. ×220 000

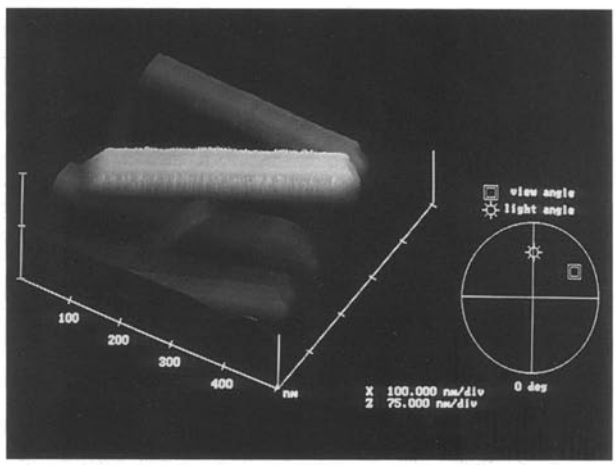

Figure 3 SFM image of rod-like tabular microcrystals of CPPD from a mixed OA deposit in r. synovium. Repulsive force image. ×113 000.

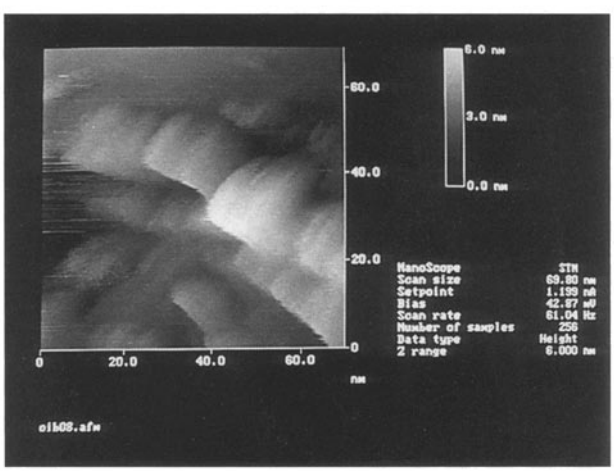

Figure 2 STM image of a mid area of Fig. 1. HA platelets, bearing a strong resemblance to those seen in calcifying collagen fibrils. Top view. 0.1 nA tunnel current, 800 mV bias. ×710 000

themselves composed of platelets. They strongly resemble STM images of synthetic hydroxyapatite. Fig. 2 is a fourfold enlargement of an area near the centre of Fig. 1. Here the small platelets are well resolved. The plate or scale-like crystals are individually some 20–30 nm long and have striations on the surface of a few nanometres in size. The resemblance to the HA platelets derived from intra-fibrillar collagen sites in calcifying turkey tendon collagen [12] is very close.

Crystals having the features of CPPD can also be identified from the mixed deposits in joints tissues. Fig. 3 shows the SFM image of small, regular tabular to rod-like crystals from the same lateral meniscus, about 400 nm in length by about 70 nm across. Much larger crystals are commoner; Fig. 4 shows the surface detail in a 1.7 μm square of a larger crystal of similar overall shape, also from a lateral meniscus. It is possible to scan these surfaces at greater resolution. Fig. 5 is a three-dimensional display of a 700 nm square of the surface in Fig. 4. This demonstrates an unexpected roughness on a scale of a few nanometres.

In order to discern if this feature was found only on disease-state crystals, where it could be the result of some etching process during the cleaning procedures, we turned our attention to pure synthetic triclinic CPPD. When the surfaces of suitable small examples of these crystals were examined in detail, a similar surface roughness could be seen, as is shown in Fig. 6. Image analysis was carried out on the Nanoscope III system for several such images. An example section

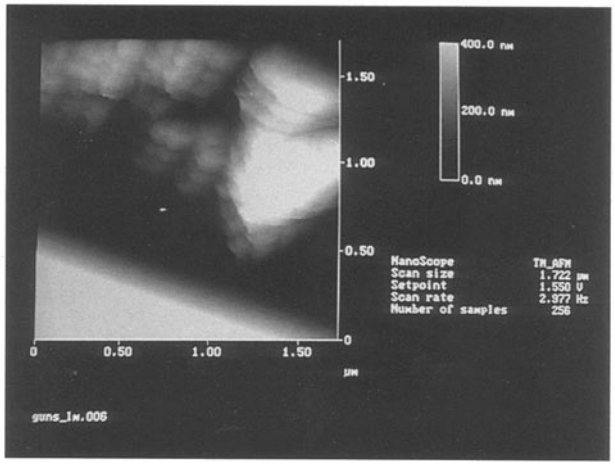

Figure 4 SFM image of edge of a larger crystal CPPD deposit in OA l. lateral meniscus. "Tapping mode" image. × 33 300.

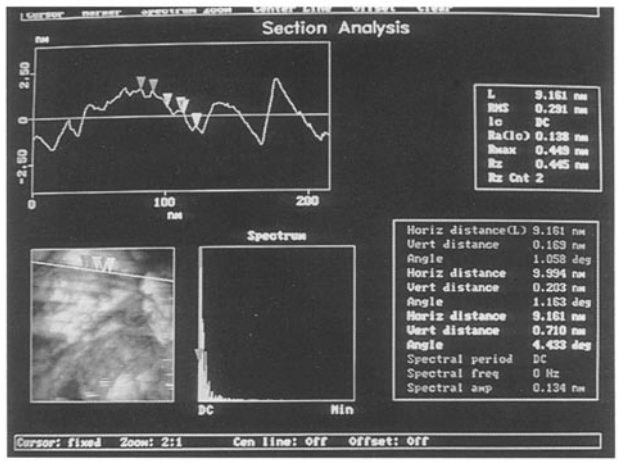

Figure 7 Section analysis of a line drawn through Fig. 6. The two depressions indicated have lateral dimensions between 14 and 16 nm and depths of about 3 nm.

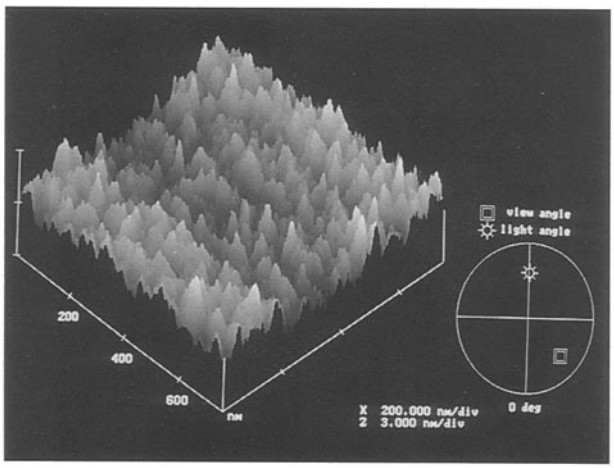

Figure 5 SFM image of surface features on a restricted area of a CPPD crystal from mixed OA deposit in l. lateral meniscus, as in Fig. 4. Surface plot showing surface roughness. "Tapping mode" image. × 75 000.

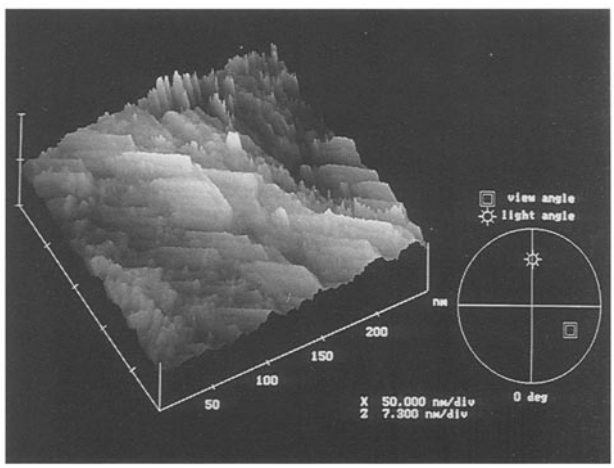

Figure 8 Surface plot of an STM image of fibronectin treated synthetic T-CPPD. Surface crystal planes can be seen along with globular deposits of protein.

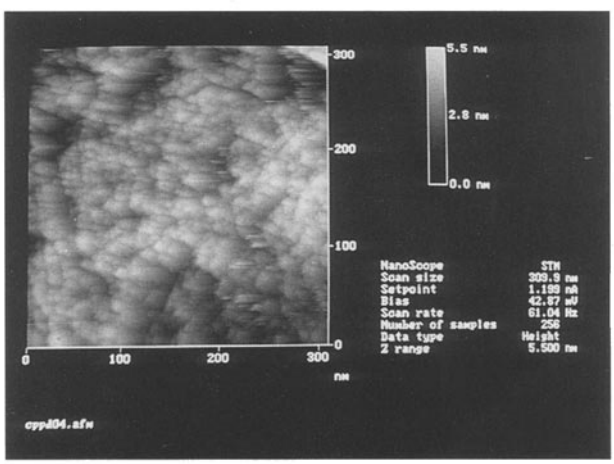

Figure 6 STM image of surface features on a synthetic T-CPPD crystal. Max. depth of features indicated as 5.5 nm. Tunnel current 0.1 nA, bias 800 mV Top view. × 227 000.

analysis on the image in Fig. 6 is shown in Fig. 7. This indicates that the surface undulations are fairly regular. The distances between markers, indicating lateral extent of the surface pits, are around 10–15 nm. Roughness analysis indicated a depth to the pits of the order of 3 nm. Fractal analysis gave a scaled dimension of 2.3, indicating a very high level of roughness on the scale investigated.

A roughness on the scale discovered, suggests immediately that the surface features are compatible with locating most globular proteins, which have a diameter of the order of 10 nm. We incubated the CPPD crystals with human serum albumin, IgG and fibronectin as described. The crystals were then re-examined by SPM to discover whether any protein molecules could be seen adhering to the crystals. Globular bodies of the expected sizes were readily detected adhering to the crystal surfaces, for the specimens of fibronectin, IgG and albumin treated CPPD. Fig. 8 is a three-dimensional representation of an area of fibronectin treated CPPD about 250 nm square, where crystal surface features are apparent along with interspersed globular material. Fig. 9 is a magnified top view of globular protein molecules decorating an area of fibronectin-treated CPPD, and demonstrates several interesting features. The area seems to be covered with parallel arrays of elliptical bodies some 30 nm × 15 nm, which in many cases can be resolved as stacks of smaller elliptical forms, with axes of the

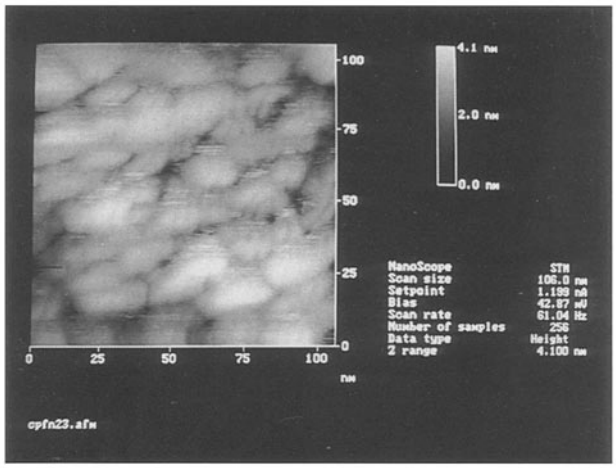

Figure 9 STM image of fibronectin adsorbed to synthetic T-CPPD surface the impression is of possibly linked ellipsoids, oriented with major ellipse axis perpendicular to the crystal surface. 0.1 nm tunnel current, 800 mV bias. × 550 000.

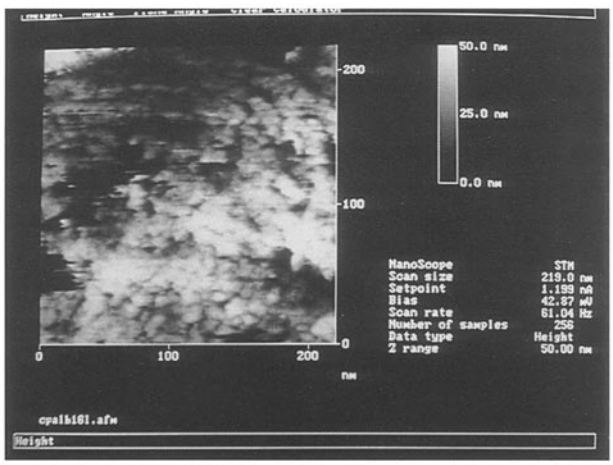

Figure 10 STM image of human albumin bound to synthetic T-CPPD. 0.1 nA tunnel current, 800 mV bias. × 265 000.

order of 10–15 nm × 5–7 nm. The major axes of these smaller components seem to be perpendicular to those of the larger bodies. It is unclear yet whether these small ellipsoids represent the molecules or subunits of the fibronectin. What is clear is that the crystal surface appears capable of attaching and organizing a protein layer, possibly a monolayer.

The STM images of albumin treated CPPD (Fig. 10) and IgG treated CPPD (Fig. 11) both also show evidence of attached protein, though less well-resolved than the fibronectin images. Globular bodies of circular or elliptical profile are seen in most regions of Fig. 10, and particularly in the lower right area of Fig. 11.

4. Discussion

There is much controversy surrounding the nature of the surfaces of arthropathic crystals and how and why they adsorb proteins and what consequences this has in OA. Specifically there is a debate on whether or not this protein adsorption contributes to the disease process, or may be a largely beneficial scavenging action,

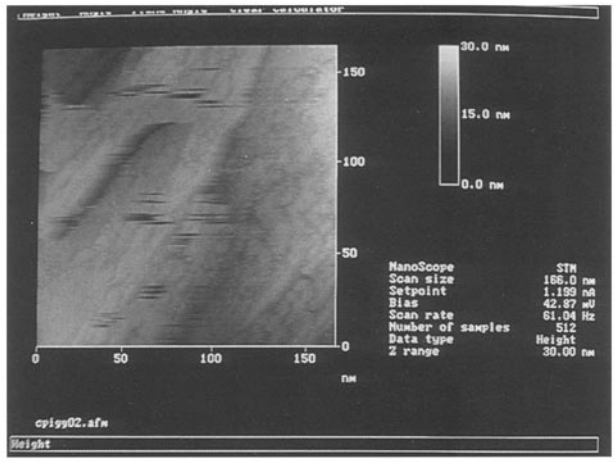

Figure 11 STM image of human IgG bound to the surface of T-CPPD, here again the attached bodies (see especially lwr.R.area), i.e. the proteins are of the correct order of size. 0.1 nA tunnel current, 800 mV bias.

particularly in synovial fluid. In this latter scenario, the mineral crystals could be seen as removing from circulation, in SF, active mediators of the disease process such as cytokines and growth factors by adsorbing them onto their surface [18, 19]. Microcrystals, having a larger surface: mass ratio would be relatively more effective in this than large crystals.

Another analysis might involve the transport and subsequent release of active proteins in high local concentrations. This would occur when the crystals became involved in a biomechanical degradative process in the joint. Release of the proteins might also occur when the crystals were wholly or partially ingested by macrophages. Release of activators of complement could also occur. Thus both HA and CPPD could contribute to the disease progression by inflammatory and biomechanical routes.

It has long been known [1, 20–22] that the calcium-containing crystals in joint tissues (especially HA) have an avidity for proteins. Indeed, HA is used as a protein binding chromatography medium. The present finding that some HA crystals from cartilage deposits closely resemble the intrafibrillar plates from calcified turkey tendon collagen suggests that, at least in some cases, the HA in these calcified sites in joint tissues had their origin within collagen fibrils, and could have become translocated by overgrowth or abrasion.

However, the present images of CPPD surfaces show for the first time, in both synthetic T-CPPD and disease-state CPPD deposits, roughness on the scale of individual protein molecules. This could help to explain their reactivity. "Rough" crystal surfaces [23, 24] have long been claimed to be inherently and directly inflammatory. Such features have never been revealed in high resolution SEM studies, at an order of magnitude lower resolution than here. A contributory effect is probably that the heavy metal coating necessary for making the specimen conductive would tend to fill the shallow pits on the surface preferentially, thus leading to a flattened effect. The overall effect would be for SEM to show a smooth surface.

Positive imaging of the proteins on the crystals confirms they are adhering to the crystal faces. In the case of the fibronectin images, there appeared to be orientational effects, suggesting a non-random, specific interaction of surface charges on the crystal with some part of the protein molecule. It is possible that the binding process to the crystal may effect non-bound regions of the exposed molecule leading to altered reactivity of the protein. Again, this could have implications for the disease process.

5. Conclusions

We have been able to demonstrate the mixture composition of crystals in knee joint OA deposits using rapid collection of diffraction data on a two-dimensional detector, and to examine the surfaces of individual microcrystals in these deposits at the resolution of about 1 nm using scanning tunnelling microscopy (STM) and scanning force microscopy (SFM). The latter methods demonstrated a roughness related to pitting on the scale of 10 nm × ~3 nm on the surface of CPPD crystals from disease origin and synthetic T-CPPD. Fibronectin, IgG and albumin incubated with synthetic TCPPD could be visualized adhering to the surface of these microcrystals. The roles of crystals in OA joints may well be surface dependent. Until now exploration of these aspects has been hindered by difficulties in identifying the mineral types in joint deposits and lack of a method for examining the particles involved and their surfaces at sufficient resolution. We hope these methods will prove to be useful in the future in further elucidating the role of crystals in joint diseases.

Note in proof

A recent SEM study of the structure of the calcite (1014) surface in aqueous solution states that the dissolution process proceeds by the creation of shallow surface pits on a nanometre scale. This raises the possibility that such surface features may be common in calcium salts [25].

Acknowledgements

This work has been supported by MRC project grant no. G9415154MA. The authors thank Dr R. P. Shellis, MRC Dental Unit, Bristol, for specimens and valuable discussion.

References

1. P. A. DIEPPE and P. CALVERT, "Crystals and joint disease" (Chapman and Hall, New York and London, 1983).
2. P. A. DIEPPE and I. WATT, *Clin. Rheum. Dis.* **11** (1985) 367.
3. D. J. McCARTY, J. R. LEHR and P. B. HALVERSON, *Arthritis and Rheum.* **26** (1983) 1220.
4. F. KOZIN and D. J. McCARTY, *J. Lab. Clin. Med.* **89** (1977) 1314.
5. R. TERKELTAUB, A. J. TENNER, F. KOZIN and M. H. GINSBERG, *Arthritis Rheum* **26** (1983) 775.
6. K. D. BRANDT and H. R. SCHUMACHER, *Curr. Opinion in Rheumatol.* **6** (1994) 429.
7. K. P. H. PRITZKER, *ibid.* **6** (1994) 442.
8. A. J. SWAN, B. R. HEYWOOD and P. A. DIEPPE, *J. Rheumatol.* **19** (1992) 1764.
9. A. J. SWAN, B. CHAPMAN, P. HEAP, H. SEWARD and P. DIEPPE, *Ann. Rheum. Dis.* **53** (1994) 467.
10. K. P. H. PRITZKER, P. T. CHENG and M. E. ADAMS, *J. Rheumatol.* **5** (1978) 469.
11. L. J. GATHERCOLE, M. J. MILES, T. J. McMASTER and D. F. HOLMES, *J. Chem. Soc. Faraday Trans.* **89** (1993) 2589.
12. D. ERTS, L. J. GATHERCOLE and E. D. T. ATKINS, *J. Mater. Sci. Mater. Med.* **5** (1994) 200.
13. O. MARTI and M. AMREIN (eds), "STM and SFM in biology" (Academic Press, San Diego, 1993).
14. C. BUSTAMENTE, D. A. ERIE and D. KELLER, *Curr. Opinion in Struct. Biol.* **4** (1994) 750.
15. R. GUCKENBERGER, M. HEIM, G. CEVC, H. F. KNAPP, W. WIEGRABE and A. HILLEBRAND, *Science* **226** (1994) 1538.
16. R. A. GATTER and H. R. SCHUMACHER, "Practical handbook of joint fluid analysis", 2nd edition (Lea and Febiger, Philadelphia and London, 1991).
17. D. J. McCARTY, *Arthritis Rheum.* **19** (1976) 275.
18. R. TERKELTAUB, L. K. CURTISS, A. J. TENNER and M. H. GINSBERG, *J. Clin. Invest.* **73** (1984) 1719.
19. C. J. ROBERGE, R. de MEDICIS, J.-M. DAYER, M. ROLA-PLESZCZYNSKI, P. H. NACCACHE and P. E. POUBELLE, *J. Immunol.* **152** (1994) 5485.
20. C. E. KEEN, P. R. CROCKER, K. BRADY, N. HASAN and D.A. LEVISON, *Histopathology* **19** (1991) 529.
21. M. KAM, D. PERL-TREVES, D. S. CASPI and L. ADDADI, *Federation of American Societies for Experimental Biology J.* **6** (1992) 2608.
22. A. BEUTLER, S. ROTHFUSS, G. CLAYBURNE, M. SIECK and H. R. SCHUMACHER, *Arthritis Rheum.* **36** (1993) 704.
23. F. KOZIN and D. J. McCARTY, *ibid.* **19** (1976) 433.
24. N. S. MANDEL, *ibid.* **19** (1976) 439.
25. Y. LIANG, D. R. BAER and J. M. McCOY, Presented at the American Vacuum Society Annual Conference, October 1995 (Minneapolis).

Received 28 June
and accepted 7 September 1995